Visible Hyperspectral Imaging for Standoff Detection of Explosives on Surfaces

Bruce E. Bernacki*, Thomas A. Blake, Albert Mendoza, and Timothy J. Johnson

Pacific Northwest National Laboratory, P.O. Box 999, Richland, WA 99352

ABSTRACT

There is an ever-increasing need to be able to detect the presence of explosives, preferably from standoff distances of tens of meters. This paper presents an application of visible hyperspectral imaging using anomaly, polarization, and spectral identification approaches for the standoff detection (13 meters) of nitroaromatic explosives on realistic painted surfaces based upon the colorimetric differences between tetryl and TNT which are enhanced by solar irradiation.

Keywords: explosives detection, standoff explosives detection, visible hyperspectral imaging

1. INTRODUCTION

In recent years explosives have become a threat not only on the battlefield, but now also pose an ever-increasing threat to civilian peoples and targets. Thus, the ability to detect and identify explosives has become far more pressing. In particular, the need to protect civilian and military personnel from improvised explosive devices (IEDs) has become a top priority across the globe. To that end, several efforts are under way for reliable detection schemes with low false positive rates for the detection of many explosives, both *in situ* and as remote sensing techniques. There are several productive regions of the electromagnetic spectrum and many methods that have been suggested for both remote and standoff detection of explosives including the millimeter wave, the terahertz (THz), the mid-infrared (IR)[1,2], and the UV-visible as well as x-ray techniques.[3,4] Nitroaromatic explosives such as TNT (2,4,6-trinitrotoluene; CAS No. 118-96-7) and tetryl (2,4,6,N-tetranitro-N-methylaniline; CAS No. 479-45-8) produce a number of colored photodecomposition products[5] and although the visible portion of the spectrum is not as feature-rich as those that reveal the molecular structure of the explosives, we show that the subtle colorimetric differences between tetryl and TNT, especially after the explosives are exposed to solar radiation, may be exploited as an additional detection path. The detection scenario described here is of explosive stains on a white car door and though the stains are fairly large (18 cm diameter) and have a generous areal dosage (~50 μg/cm^2), with better optical matching between the imaging spectrometer and the detection surface we're confident that smaller and less concentrated stains can be detected with this method.

2. EXPERIMENTAL

2.1 Visible Hyperspectral Imager

The experimental apparatus consists of a visible hyperspectral imager based upon a concentric[6] or Offner-type design which is commercially available.[7] The F/2 push broom imager is mated to a 1392 (spatial) × 1040 (spectral) pixel single-stage thermo-electric-cooled visible silicon camera having 6.45 μm square pixels. The device has a spectral resolution of ~3 nm with the 12 μm input slit with 18 mm height, and was equipped with a 35 mm focal length lens that was aberration-corrected for the entire 400-1000 nm sensitivity range of the sensor. The lens was also coated with a broadband anti-reflection coating to ensure a transmittance greater than 90% throughout the sensitivity range of the spectrometer.[8] In order to create two-dimensional spatial images using a fixed imaging position, a scanning mirror was integrated with the imager to build up an image of the scene. All data were taken with a ground separation distance of

* bruce.bernacki@pnl.gov; phone 509-375-2135

Optics and Photonics for Counterterrorism and Crime Fighting VI and Optical Materials in Defence Systems Technology VII, edited by Colin Lewis, Douglas Burgess, Roberto Zamboni, François Kajzar, Emily M. Heckman,
Proc. of SPIE Vol. 7838, 78380C · © 2010 SPIE · CCC code: 0277-786X/10/$18 · doi: 10.1117/12.870739

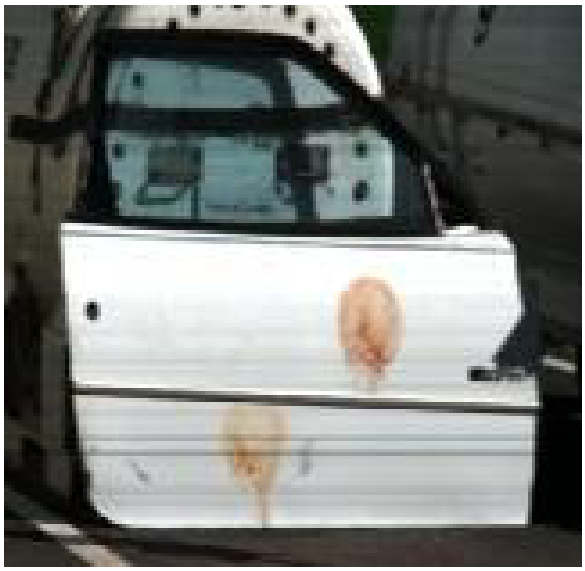

Figure 1. An image of the automobile car door showing the TNT (upper right) and tetryl (lower left) stains. The 42 μg/cm^2 TNT stain is visible on the upper right metal portion of the door and the 37 μg/cm^2 tetryl stain is visible in the center of the lower portion of the door. An 81 μg/cm^2 RDX stain is to the left of the TNT stain, but is not visible.

13 m between the imager and the car door. Four hundred and sixty three bands of spectral data were recorded. The door was held in a vertical orientation and was illuminated by ambient sunlight.

2.2 Sample Preparation

In order to provide a relevant sample surface, a white-painted automobile door was obtained from an automobile wrecking yard and the tetryl, TNT, and RDX stains were applied to the door using solutions of these compounds in acetonitrile. A large piece of cardboard with an 18 cm diameter cutout was used as a mask and placed over the door. The solution to be applied was poured into a spray bottle, tared on a balance, and then sprayed over the cutout. The solvent was allowed to evaporate, the solution and spray bottle weighed, and the mass of deposited explosive compound determined. Two stains were applied to the upper half of the car door's metal surface: an 81 μg/cm^2 RDX stain on the

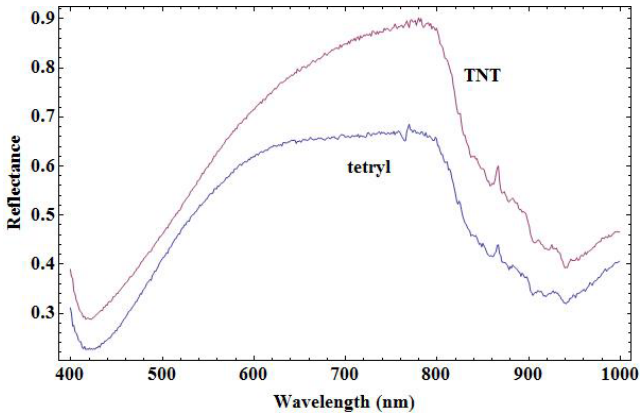

Figure 2. Spectral end members extracted from the hyperspectral image for TNT (upper red trace) and tetryl (lower blue trace) stains.

left side and a 42 μg/cm^2 TNT stain on the right (Figure 1). On the lower half of the door's metal surface a 37 μg/cm^2 aliquot of tetryl was applied. The glass has an 87 μg/cm^2 RDX stain on the left and a 46 μg/cm^2 TNT stain on the right. A color image of the automobile passenger door is shown in Figure 1 produced by mapping spectral images recorded at 649.9 nm, 531.8 nm and 486.4 nm into red, green and blue display colors. Spectralon® reference surfaces are incorporated into the scene (not shown) that provide calibrated reflectance values of 99% and 20% respectively so that the wavelength and transmission variations inherent in the optics, dispersive grating, camera focal plane and solar radiation can be removed prior to analysis. An empirical line correction approach was taken to calibrate the reflectance images.[9] Spectral end members that were extracted from the hyperspectral image of the car door seen in Figure 1 can be seen in Figure 2. All analysis was carried out using ENVI, a commercial hyperspectral image processing software package.[10]

3. RESULTS

3.1 Anomaly Detection

Principal component analysis (PCA) is often used in hyperspectral imaging to reduce the dimensionality of a data set and to produce uncorrelated output bands.[11] As a result of the transformation the data is reordered with regard to the amount of variance in each component. That is, the transform operates on the original image with a high degree of correlation and produces components after the transform that are uncorrelated with respect to each other, and are rank-ordered according to the amount of signal variance contained in them. The PC1 component has the highest degree of variance, and is basically the intensity image, while the latter components have reduced variance and appear noisier. In Figure 3 a selection of principal components is shown to illustrate the feature enhancement that can occur due to the transformation. To make the features further apparent to a human observer, principal component images are mapped into the red, green and blue of a color display. In this example, PC6, PC7, and PC8 are mapped respectively, thus highlighting the subtle differences between the TNT (upper right), and the tetryl (lower left) stain. Note that in Figure 4 a barely discernable outline of an additional stain can be seen, which is due to RDX, which dries to a white, microcrystalline powder when deposited from solution.

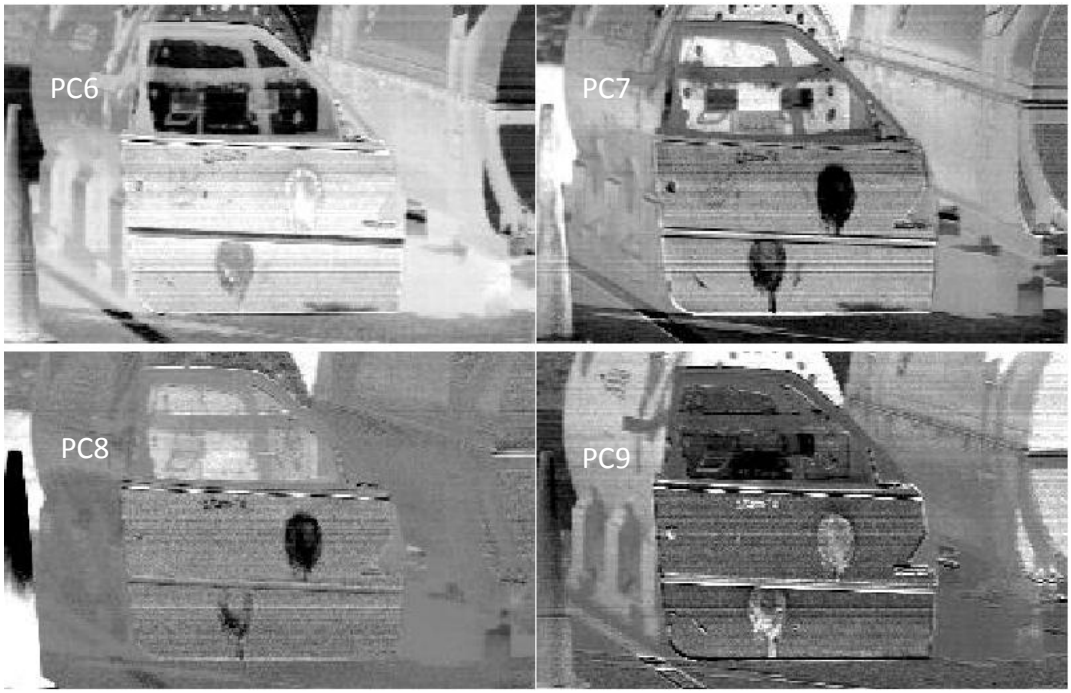

Figure 3. A selection of principal component (PC) images, from PC6 through PC9.

Figure 4. Shown above is a color mapping of PC components 6, 7, and 8 into the red, green and blue display colors, respectively. Note that the outline of the RDX residue patch is also visible in the image that is not apparent in a normal intensity image.

3.2 Polarization Imaging

An additional anomaly detection approach was employed using polarization imaging. Images were recorded using the

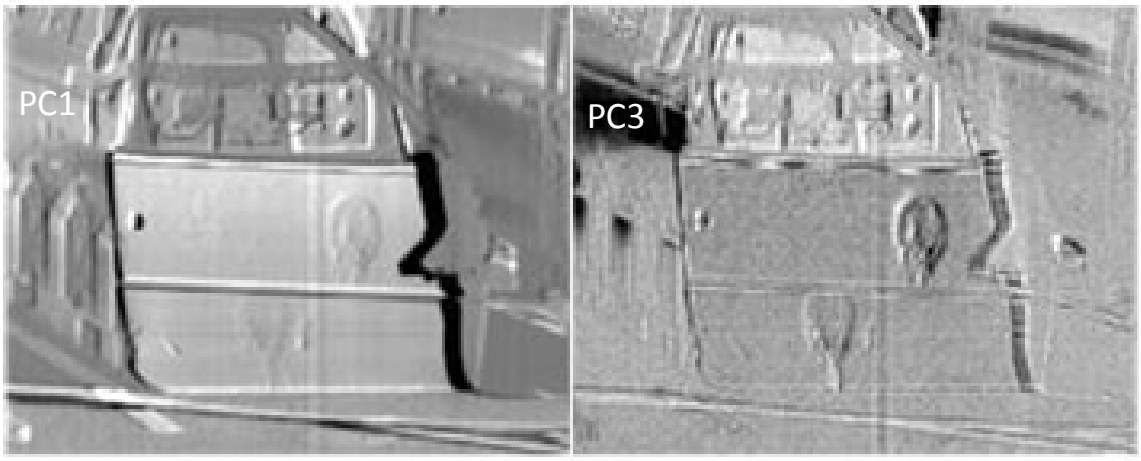

Figure 5. PC components 1 and 3 are shown that reveal the scattering from the TNT (upper) and tetryl (lower) stains on the car door. The RDX residue was not evident in any of the Q image components or subsequent principal component transform.

hyperspectral camera that was equipped with a broadband polarizer in front of the imaging lens. Two images were recorded with the polarizer oriented in the zero degree position (horizontal, H) and in the 90 degree position (vertical, V). From this the I and Q Stokes images were calculated.[12] The I, or intensity, image is the sum of the H and V hyperspectral images. The Q image is the difference between the H and V images and describes the tendency of the signal to contain signals with polarization orientated preferentially with either the horizontal or vertical polarization axes. To further highlight the polarization features that resulted in the Q image, a Principal Component transform was used to further operate on the Q image data, which resulted in the images shown in Figure 5. PC1 faintly reveals the location of the TNT and tetryl stains. However, PC3 demonstrates enhanced detection of the stain due to the partial polarization of the reflected solar radiation after its interaction with the car door and explosive residue.

3.3 Spectral Identification

Anomaly detection methods such as PCA allow one to highlight the presence of features that are clustered spectrally, but there is no spectral identification *per se*. Spectral methods include approaches such as least squares (spectral feature fitting), matched filtering, mixture-tuned matched filtering, and orthogonal subspace projection, to name a few.[13] These methods are included in ENVI and were applied using the extracted end members shown in Figure 2, but only mixture tuned matched filtering showed marked differentiation between the TNT and tetryl stains. No spectroscopic methods could detect the RDX residue using the visible hyperspectral imager.

Mixture tuned matched filtering (MTMF) is a form of matched filtering (MF) that adds an infeasibility image to the calculation results, in addition to the score image. The score image pixel values indicate the relative abundance of the detected target material. The infeasibility image is a measure of the signal-to-noise ratio in the matched filtering operation, and when combined with the MF score image, allows one to reduce the number of false positives in the calculation results when compared with a simple MF approach. ENVI reports the infeasibility values in noise sigma units. Since the MTMF algorithm in ENVI requires an input with unit variance noise, one must first apply the minimum noise fraction (MNF) transform prior to using the MTMF function. The MNF transform in ENVI is based upon an approach by Green *et al*[14] that is related to principal component analysis (PCA), but ranks the resulting transformed

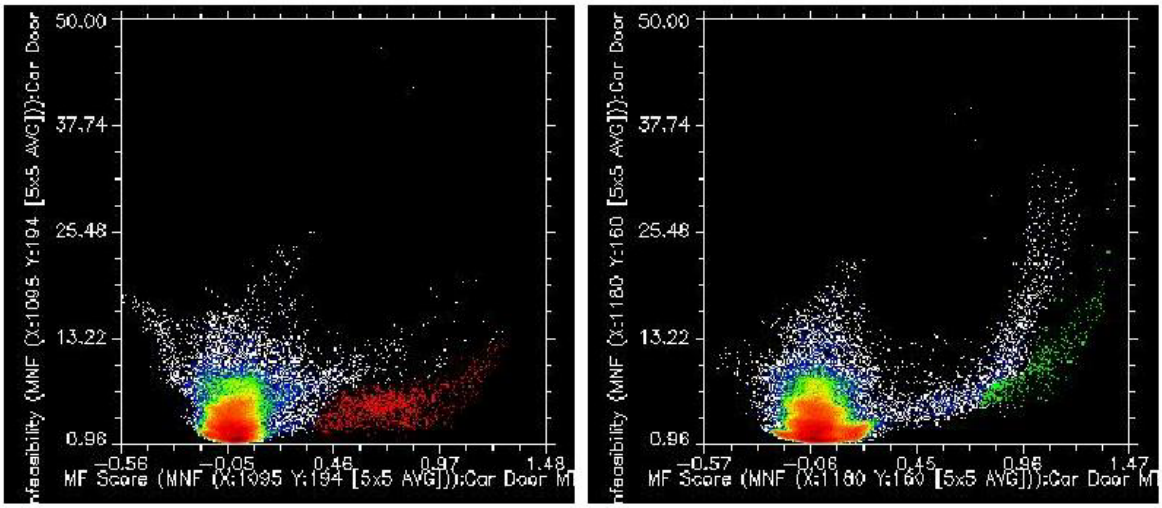

Figure 6. 2D scatter or score plots of the infeasibility image versus the score image for the TNT (left) and tetryl (right) stains on the car door. One can interactively select those pixels in the score plots above that satisfy criteria for high MF score - low infeasibility to reduce false positives. The pixels selected are color coded by class and correspond to image pixels meeting these criteria. In this case the red pixels highlighted in the lower right-hand corner of the TNT scatter plot (left) classify the presence of TNT, while the green pixels highlighted in the lower right-hand corner of the tetryl scatter plot (right) correspond to tetryl content on the car door surface.

images in terms of noise content. PCA, in contrast, ranks the images according to the amount of data variance they contain. As was mentioned previously, PCA is used to reduce the dimensionality of hyperspectral data sets, produce uncorrelated output bands, and segregate noise, although the noisy components do not always correlate with increasing component number. MNF has also been described as the noise-adjusted principal component transform which ensures that the components are rank ordered with respect to noise content.

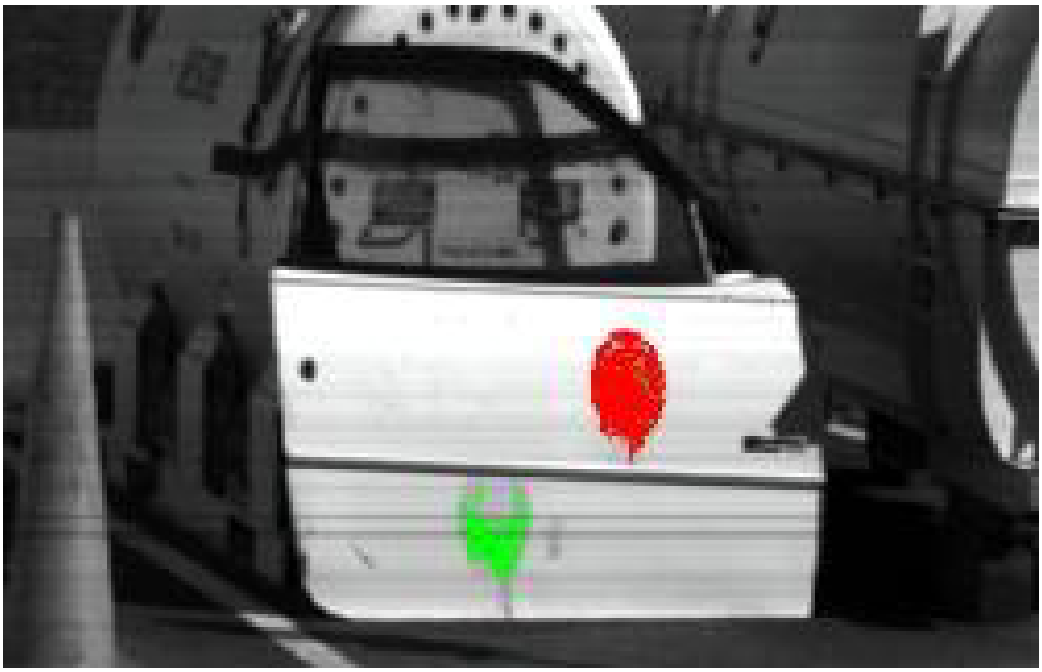

Figure 7. Classification image of the car door after the MTMF operation and selection of target pixels that meet the dual criteria of high score – low infeasibility interactively using the 2D score plots. The red pixels selected from the score plot show the location of the TNT residue on the car door, while the green pixels show the location of the tetryl residue.

After applying the MNF transform, the noise and signal components are separated by only using those MNF transform components whose eigenvalues have a value greater than unity. The matched filtering then operates on only the subset of MNF components or so-called coherent images that demonstrate good signal to noise. The reference spectra seen in Figure 2 must also be transformed into MNF space prior to this operation. To find target areas that are matched to the reference spectra, the resulting score and infeasibility images are viewed in a 2D scatter or score plot to select those pixels that satisfy the dual criteria of high matched filter score - low infeasibility (or low noise). The score plots are shown in Figure 6. ENVI has provisions to accomplish this interactively by selecting these pixels from the score plot. The selected region is color-coded by class and the corresponding pixels in the image that are members of this class are depicted with the same color. One prominent advantage of the MTMF approach is its ability to only use MNF components that have eigenvalues greater than the noise floor to enhance the sensitivity of detection. In this example, 15 MNF components were retained for use in the MTMF operation. The classified image that results from the selection of high score – low infeasibility pixels for each target species is shown in Figure 7.

4. SUMMARY AND CONCLUSIONS

The nitroaromatic compounds TNT and tetryl photodecompose with solar exposure into compounds that have subtle, but distinct visible wavelength spectra and we have presented an application of visible hyperspectral imaging to identify and locate these explosive residues on a car door at a standoff distance of 13 meters. Using extracted spectral end members

from the visible hyperspectral images, anomaly detection (including polarization imaging) and spectral identification methods were both applied with success. PCA was shown to reveal the location of the TNT and tetryl residue, as well as showing the faint presence of RDX residue that was not visible at all in the conventional color or grayscale images. Polarization imaging exploits the interaction of solar radiation with anisotropic surfaces, and PCA on the resulting Q image highlighted the location and presence of suspicious stains at the locations corresponding to the TNT and tetryl residues. Finally, mixture tuned matched filtering was used to spectrally identify and locate the presence of the TNT and tetryl residue with a high degree of certainty in spite of the subtle (to the eye) color differences between the two explosive residues. Although not as specific as spectroscopic approaches[15,16] that exploit the fundamental molecular signatures of explosives,[17] visible hyperspectral imaging including polarimetric imaging may offer an orthogonal detection method due to the relatively low cost of components and cameras when compared to other spectral regions and when used in conjunction with bulk or trace detection methods for the screening of motor vehicles or cargo for the presence of explosives.

4. ACKNOWLEDGMENTS

The research described in this paper was conducted under the Laboratory Directed Research and Development Program at Pacific Northwest National Laboratory, a multiprogram national laboratory operated by Battelle for the U.S. Department of Energy under Contract DE-AC05-76RL01830.

REFERENCES

[1] Blake, T.A., J.F. Kelly, N.B. Gallagher, P.L. Gassman, and T.J Johnson, "Passive standoff detection of RDX residues on metal surfaces via infrared hyperspectral imaging," Anal. Bioanl. Chem., 395, 337-348 (2009).
[2] Bernacki, B. E., Phillips, M. C., "Standoff hyperspectral imaging of explosives residues using broadly tunable external cavity quantum cascade laser illumination," Proc. SPIE **7665**, 76650I (2010).
[3] Yinon, J., [Counterterrorist Detection Techniques of Explosives], Elsevier, New York, (2007).
[4] Yinon, J., [Forensic and Environmental Detection of Explosives], Wiley, New York, (1999).
[5] Becker, N.M., "Fate of Selected High Explosives in the Environment: A Literature Review" Los Alamos National Laboratory Report LA-UR-95-1018 (1995).
[6] Fisher, J. M Baumback, J. Bowles, J. Grossman, and J. Antoniades, "Comparison of low-cost hyperspectral sensors," Proc. SPIE **3438**, 0277-786X (1998).
[7] Hyperspec™ VNIR C-series imaging spectrometer, http://www.headwallphotonics.com
[8] http://www.schneideroptics.com
[9] van der Meer, F.D, and S.M. de Jong, Ed., [Imaging Spectrometry], Springer-Verlag, Dordrecht, (2006).
[10] http://www.ittvis.com
[11] Richards, J.A. and X. Jia, [*Remote Sensing Digital Image Analysis – 4th Ed.],* Springer-Verlag, Berlin, (2006).
[12] Schott, J.R., [*Fundamentals of Polarimetric Remote Sensing],* SPIE Press, Bellingham, WA, (2009).
[13] Anonymous, [*ENVI User's Guide*], ITT Visual Information Solutions, (2009).
[14] Green, A.A., M. Berman, P. Switzer, and M.D. Craig, "A Transformation for Ordering Multispectral Data in Terms of Image Quality with Implications for Noise Removal" *IEEE Trans. Geos. Remote Sensing* **26**, 65-74 (1988).
[15] Sharpe, S.W. R.L. Sams, T.J. Johnson, P.M. Chu, G.C. Rhoderick, and F.R. Guenther, "Creation of 0.10 cm^{-1} Resolution, Quantitative, Infrared Spectral Libraries for Gas Samples," Proc. *SPIE* **4577**, 12-24 (2001).
[16] Sharpe, S.W. T.J. Johnson, R.L. Sams, P.M. Chu, G.C. Rhoderick P.A. Johnson, "Gas-phase Databases for Quantitative Infrared Spectroscopy," *Appl. Spectrosc* **58,** 1452-1459 (2004).
[17] Sharpe, S.W., T.J. Johnson, D.M. Sheen, and D.A. Atkinson, "Relative Infrared (IR) and Terahertz (THz) Signatures of Common Explosives." Proc. SPIE **6378**, 63780A (2006).